Mechanical properties and temperature dependence of B19 $Ti_{50-x}Zr_xPt_{50}$ shape memory alloys

M P Mashamaite[1], H R Chauke[1] and P E. Ngoepe[1]

[1]Materials Modelling Centre, School of Physical and Mineral Sciences, University of Limpopo, Private Bag X1106, Sovenga 0727, South Africa

Email: mordecai.mashamaite@ul.ac.za, mordecai.mashamaite@gmail.com

Abstract. A molecular dynamic study of $Ti_{50-x}Zr_xPt_{50}$ as potential high temperature shape memory alloy has been performed using the LAMMPS code. The lattice dynamics, elastic properties and temperature dependence were deduced to determine the effect of ternary addition with Zr on the Ti sub-lattice at varied temperature range. It was found that the lattice parameter increases with Zr addition, the thermodynamic stability was observed at 5 at. % Zr. Furthermore, the elastic properties showed positive shear modulus for concentrations range 5 - 25 at. % Zr, indicating stability of the structures and instability above 25 at. % Zr concentrations. More importantly, we observed a martensitic transformation behaviour for $Ti_{50-x}Zr_xPt_{50}$ (x= 5.56) at around 1200 K.

1. Introduction

Shape memory alloys (SMAs) design & applications has found commercial use in a broad range of industries including automotive, aerospace, robotics and biomedical [1]. These alloys are able to remember their shape after being deformed when heated above certain temperatures. The practical uses for SMAs are limited to temperature below 373 K [2]. Various alloys such as NiTi, NiAl, TiPd and TiAu have been investigated, amongst them NiTi-based SMAs have been used extensively in industries because of its resistance to corrosion and the fact that the martensitic transformation temperature (Ms) is near room temperature. TiPd undergoes a B2-to-martensite phase transformation with a Ms between 780 and 836 K [2, 3]. However, studies reveal that TiPd exhibits extremely poor shape-memory behavior with little recoverable strain during transformation, even under no-load conditions, which is attributed to a low critical stress for slip in the alloy [4].

A limited number of alloys have potential as high-temperature shape memory alloys (HTSMAs). Hence, HTSMAs are being developed in order to increase the application areas of shape memory alloys [5]. Interest in HTSMA has been growing in the aerospace, automotive, process control and energy industries. One way to increase the transformation temperature is to add significant levels of particular ternary additions [6] which were found to be effective for increasing the transformation temperature [7]. Hence, NiTi-X (X=Pt, Pd, Hf and Zr) shape memory alloys have been studied for high temperature above 373 K applications [8, 9]. However, TiPt has a higher Ms of above 1273 K rendering it suitable for the development of HTSMAs [2]. According to Yamabe-Mitarai et al. [10], $Ti_{50}Pt_{50}$ alloy exhibit very low shape memory effect with a recovery ratio of ~11%, however, the ratio increases between ~40% and ~60% for $Ti_{45}Zr_5Pt_{50}$ [11].

In this work Zr is partially substituted on the Ti sub-lattice of the B19 TiPt to investigate the stability of the structures in terms of their formation energies, and the elastic properties. Furthermore, the temperature dependence was investigated by studying the lattice expansion and mechanical properties of the 5.56 at % Zr structure.

2. Methodology

The first principle density functional theory (DFT) was used to study the TiPt−Zr as a potential HTSMAs, The CASTEP code [12] was employed along with the Ultrasoft pseudopotentials with a plane-wave basis set, to achieve a good convergence with respect to the total energy [13]. We have used the generalized gradient approximation (GGA) of the Perdew-Burke-Ernzerhof (PBE) exchange correlation functional [14]. The Brillouin zone integrations were performed for suitably large sets of *k*-points according to Monkhorst and Pack [15]. The energy cutoff of 500 eV and k-points mesh 8×13×8 for B19 TiPt were used in order to determine the quality of the calculations. A 2x2x1 supercell was used to generate $Zr_xTi_{50-x}Pt_{50}$ compounds by substituting Zr atoms on the Ti site. The temperature dependence calculations were evaluated utilizing molecular dynamics code based Large-scale Atomic Molecular Massively Parallel Simulator (LAMMPS) with an Embedded Atom Method (EAM) module [16] as implemented by Materials Design.

3. Results and Discussion

The equilibrium lattice parameter of the optimized structures and heats of formation are listed in Table 1. We note that our DFT predicted lattice parameters are in good agreement with available experimental and theoretical results for the binary phase. Upon doping, the lattice parameter increases with the increase in Zr content. Furthermore, the heats of formation (ΔH_f), of the intermetallic phases is calculated according to the relation [17, 18]

$$\Delta H_f = E^{TiPt} - [(1-x)E^{Ti}_{solid} + xE^{Pt}_{solid}], \quad (1)$$

where E^{TiPt}, E^{Ti}_{solid} and E^{Pt}_{solid} are the total energies of an intermetallic alloy, and elemental Ti and Pt in their respective ground-state crystal structures, while *x* and *1-x* refers to the fractional concentrations of the constituent elements. The binary B19 $Ti_{50}Pt_{50}$ heats of formation is in good agreement with the previous report. Furthermore, we see that the $Zr_5Ti_{45}Pt_{50}$ structure displayed the lowest heats of formation and is considered the most stable phase, while the $Zr_{45}Ti_5Pt_{50}$ is the least stable with values -4.858 eV/atom and 3.326 eV/atom, respectively.

Table 1 The equilibrium lattice parameters and heats of formation (ΔH_f) of B19 TiPt and B19 $Ti_{50-x}Zr_x$ Pt_{50} ternaries alloys.

B19 Composition	Lattice Parameter						(ΔH_f)
	a	Exp	*b*	Exp	*c*	Exp	
$Ti_{50}Pt_{50}$	4.633	4.550 [2]	2.791	2.730 [2]	4.876	4.790 [2]	-0.827 [19]
$Zr_5Ti_{45}Pt_{50}$	4.655		2.808		4.895		-4.858
$Zr_{10}Ti_{40}Pt_{50}$	4.677		2.825		4.917		-3.944
$Zr_{15}Ti_{35}Pt_{50}$	4.700		2.841		4.937		-2.951
$Zr_{20}Ti_{30}Pt_{50}$	4.722		2.858		4.961		-1.902
$Zr_{25}Ti_{25}Pt_{50}$	4.745		2.876		4.968		-0.831
$Zr_{30}Ti_{20}Pt_{50}$	4.766		2.893		5.013		0.220
$Zr_{35}Ti_{15}Pt_{50}$	4.787		2.912		5.043		1.225
$Zr_{40}Ti_{10}Pt_{50}$	4.807		2.926		5.08		2.205

$Zr_{45}Ti_5Pt_{50}$	4.829	3.146	5.067	3.326

Now, we consider the elastic properties to examine the mechanical stability of these alloys, for pure and doped systems. We calculated the elastic constants for B19 $Ti_{50-x}Zr_xPt_{50}$ structures, as presented in Table 2. Note that the mechanical stability in an orthorhombic crystal leads to the following restrictions:

$$(C_{11} + C_{22} - 2C_{12}) > 0;\ (C_{11} + C_{33} - 2C_{13}) > 0;\ (C_{22} + C_{33} - 2C_{23}) > 0;$$
$$C_{11} > 0;\ C_{22} > 0;\ C_{33} > 0;\ C_{44} > 0;\ C_{55} > 0;\ C_{66} > 0;\ (C_{11} + C_{22} + C_{33} + 2C_{12} + 2C_{13} + 2C_{23}) > 0 \quad (2)$$

We observe that the calculated shear moduli are positive for all structures ($Zr_5Ti_{45}Pt_{50}$, $Zr_{10}Ti_{40}$ Pt_{50}**,** $Zr_{15}Ti_{35}$ Pt_{50}, to $Zr_{25}Ti_{25}$ Pt_{50}) with less Zr concentration satisfying. The structures satisfy mechanical stability. This observation is consistent with the formation energies in table 1. The structures $Zr_{30}Ti_{20}Pt_{50}$, $Zr_{35}Ti_{15}Pt_{50}$, $Zr_{40}Ti_{10}Pt_{50}$ and $Zr_{45}Ti_5Pt_{50}$ are observed to be unstable since the C_{44} is negative. For a completely isotropic material A=1, while values smaller or greater than unity measure the degree of elastic anisotropy. The elastic anisotropy for non-cubic phases is represented by A_1, A_2 and A_3. We note that the calculated A_1 approaches unity with an increase in Zr content. On the contrary, the A_2 and A_3 calculated values are observed to decrease with increase in Zr. The bulk modulus (B) for the $Zr_{10}Ti_{40}$ Pt_{50}**,** $Zr_{15}Ti_{35}$ Pt_{50}, to $Zr_{25}Ti_{25}$ Pt_{50} structures become less in hardness with increasing Zr,

Table 2 The elastic constants (Cij) for B19 $Ti_{50-x}Zr_xPt_{50}$ structures at various concentration, 0K.

Structures	Elasticity (GPa)													
	C_{11}	C_{12}	C_{13}	C_{22}	C_{23}	C_{33}	C_{44}	C_{55}	C_{66}	C'	B	A_1	A_2	A_3
$Zr_5Ti_{45}Pt_{50}$	314	112	145	364	91	319	6	60	69	101	179	0.683	0.035	0.087
$Zr_{10}Ti_{40}$ Pt_{50}	324	117	147	368	89	321	7	62	70	103	186	0.683	0.040	0.099
$Zr_{15}Ti_{35}$ Pt_{50}	317	118	145	367	95	329	8	62	71	99	184	0.716	0.045	0.112
$Zr_{20}Ti_{30}$ Pt_{50}	310	117	148	344	94	325	6	62	71	97	182	0.739	0.035	0.084
$Zr_{25}Ti_{25}$ Pt_{50}	301	119	139	317	89	305	14	62	71	91	179	0.778	0.088	0.203
$Zr_{30}Ti_{20}Pt_{50}$	301	135	148	294	96	304	-70	62	70	83	190	0.851	0.457	1.002
$Zr_{35}Ti_{15}Pt_{50}$	287	136	141	279	94	287	-110	60	69	76	186	0.918	0.756	1.583
$Zr_{40}Ti_{10}Pt_{50}$	272	134	147	303	92	280	-25	58	69	69	180	0.996	0.193	0.364
$Zr_{45}Ti_5Pt_{50}$	267	157	143	192	101	238	-456	48	65	55	194	1.180	4.171	7.023

The effect of temperature on the lattice parameter of the B19 $Ti_{50-x}Zr_xPt_{50}$ (x=5.56) was investigated and is shown in Figure 1. We observe that the lattice parameters a and c increase linearly with temperature, while b decreases. The martensitic transformation is observed around 1200 K, this also correspond to the austenite start at around 1270 K. Above this temperature, we observed expansion of the lattice parameters, mostly the separation of a and c. The lattice ratio a/b and c/b also increases with temperature with values within 1.4 and 1.61, respectively.

Furthermore, we calculated the elastic constant at varied temperature only for the B19 $Zr_{5.56}Ti_{44.44}Pt_{50}$ (Figure 2). Most of the independent Cij satisfy the conditions of stability for the orthorhombic system, with a slight decrease as temperature is increased. The shear moduli $(C_{11} + C_{22} - 2C_{12})$ and $(C_{11} + C_{33} - 2C_{13})$ are positive from (173 K – 2073 K) temperature range, while $(C_{22} + C_{33} - 2C_{23})$ is negative above 1400 K. However, the shear moduli substantially decrease as temperature is increased. This may suggest that the structure could be stable at high temperature condition and likely to enhance the Ms.

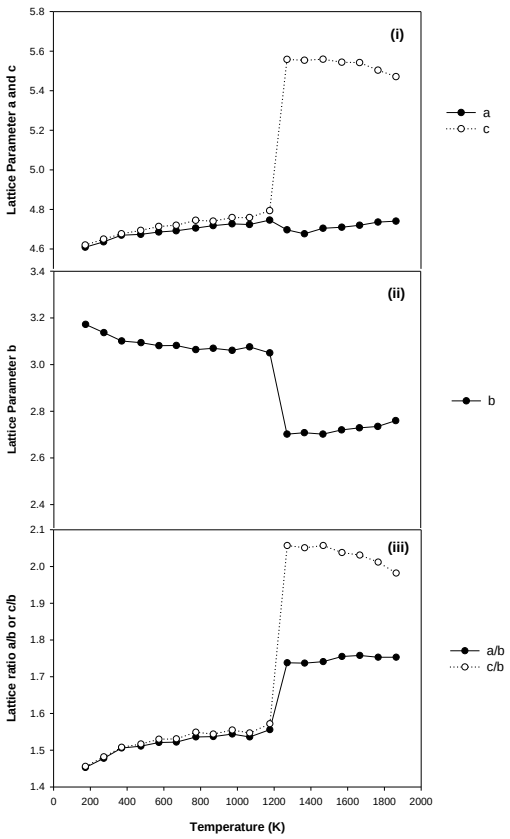

Figure 1 The effect of temperature on lattice parameter (i) a and c, (ii) b and (iii) lattice ratio a/b or c/b of B19 $Zr_{5.56}Ti_{44.44}Pt_{50}$.

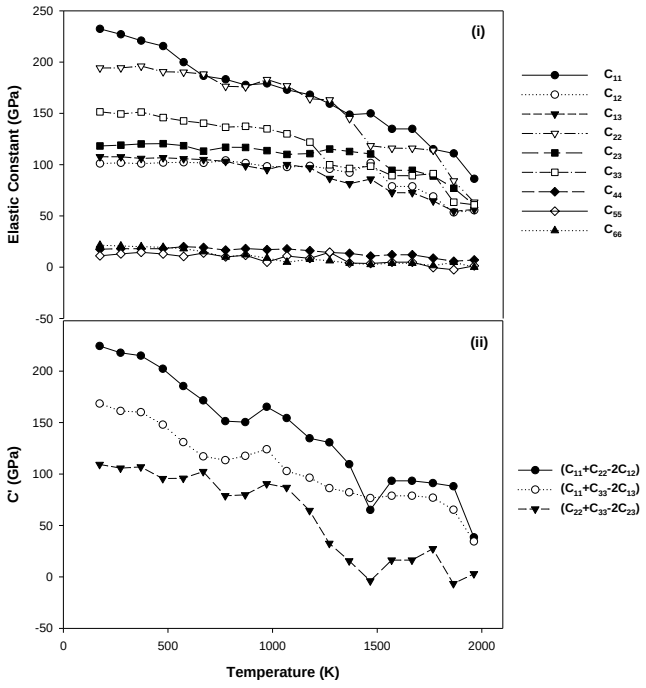

Figure 2 The graph of the (i) elastic constants and (ii) shear moduli C′ against temperature for the B19 $Zr_{5.56}Ti_{44.44}Pt_{50}$ structure.

4. Conclusion

The effect of Zr substitution was investigated on Ti sub-lattice using DFT within the generalised gradient approximations. The $Ti_{50-x}Zr_xPt_{50}$ alloys were determined by varying the concentration of Zr. We found that $Zr_5Ti_{45}Pt_{50}$ is more stable, while $Zr_{25}Ti_{25}Pt_{50}$ is the least stable. We observed that 5 – 25 at. % Zr are more stable as compared to 30 - 45 at. % Zr for elastic constant at 0 K. The temperature dependence of the lattice parameters and elastic properties was investigated within the LAMMPS-EAM code, to deduce the Ms for B19 $Zr_{5.56}Ti_{44.44}Pt_{50}$ ternaries. The B19 $Zr_{5.56}Ti_{44.44}Pt_{50}$ showed martensitic transformation above 1200 K. Interestingly, the lattice ratio c/b and a/b were calculated and found to be 1.56 and 1.57, respectively. Furthermore, it was observed that as the temperature is increased, the shear moduli decreases suggesting stability at elevated temperatures. It can be deduced that the thermodynamic and elastic stability is maintained and this may have good effect on the corrosion resistance over temperature range from 900 to 1400 K.

5. Acknowledgement

The calculations were performed at Materials Modelling Centre, University of Limpopo, South Africa. The support of the South African Research Chair Initiative of the Department of Science and Technology and the National Research Foundation is highly recognised.

References

[1] Biggs T, Cortie M B, Witcomb M J and Cornish L A 2001 Martensitic transformation, microstructure, and mechanical workability of TiPt *Metall. Mater.Trans.* **32A** 1881

[2] Donkersloot H C and van Vucht J H N 1970 Martensitic transformations in gold-titanium, palladium-titanium and platinum-titanium alloys near the equiatomic composition *J. Less-Common Metals*. **20** 83

[3] Cai W, Tanaka S and Otsuka K 2000 *Mater. Sci. Forum*. **327** 279

[4] Otsuka K, Oda K, Ueno Y, Piao M, Ueki T and Horikawa H 1993 The shape memory effect in a $Ti_{50}Pd_{50}$ alloy *Scripta Metall. Mater.* **29** 1355

[5] Ye Y Y, Chan C T and Ho K M 1997 Structural and electronic properties of the martensitic alloys TiNi, TiPd and TiPt *Phys. Rev.B* **56** 3678

[6] Sasaki T T, Hornbuckle B C, Noebe R D, Bigelow G S, Weaver M L, and Thompson G B 2013 Effect of aging on microstructure and shape memory properties of a Ni-48Ti-25Pd (At. Pct) alloy *Metall. and Mater. Trans.* **44**A 1388

[7] Ma J, Karaman I and Noebe R D 2010 High temperature shape memory alloy. *Int. Mater. Rev.* ***55*** 257

[8] Bozzolo G, Noebe R D and Mosca H O 2005 Site preference of ternary alloying additions to NiTi: Fe, Pt, Pd, Au, Al, Cu, Zr and Hf *J. Alloys. Comp.* **389** 80

[9] Firstov G S, Van Humbeeck J and Koval Y N 2004 High-temperature shape memory allloys some recent developements *Mater. Sci. Eng.* A **378** 2

[10] Yamabe-Mitarai Y, Hara T, Miura S and Hosoda H 2010 Shape memory effect and pseudoelasticity of TiPt *Intermetallics* **18** 2275

[11] Wadood A, Takahashi M, Takahashi S, Hosoda H and Yamabe-Mitarai Y 2013 High-temperature mechanical and shape memory properties of TiPt-Zr and TiPt-Ru alloys *Mater. Sci. Eng*. A**564** 34

[12] Clark S J, Segall M D, Pickard C J, Hasnip P J, Probert M J, Refson K and Payne M C 2005 Zeitschrift für Kristallographie *First-principles methods using CASTEP* **220** 567

[13] Payne M C, Teter M P, Allan D C, Arias T A, and Joannopoulos J D 1992 Iterative minimization techniques for ab initio total-energy calculations: molecular dynamic and conjugate gradients *Rev. Mod. Phys.* **64** 1045

[14] Perdew J P, Burke K and Ernzerhof M 1996 *Phys. Rev. Lett.* **77** 3865

[15] Monkhorst H J and Pack J D 1976 Special points for brillouin-zone intergrations *Phys. Rev. B* **13**

5188
[16] Nørskov J K 1979 Electron structure of single and interacting hydrogen impurities in free-electron-like metals *Phys. Rev. B* **20** 446
[17] Phasha M J, Ngoepe P E, Chauke H R, Pettifor D G and Nguyen-Mann D 2010 Link between structural and mechanical stability of fcc- and bcc-based ordered Mg-Li alloys *Intermetallics* **18** 2083
[18] Mahlangu R, Phasha M J, Chauke H R, Ngoepe P E 2013 Structural, Elastic and Electronic Properties of Equiatomic PtTi as Potential High-Temperature Shape Memory Alloy *Intermetallics* **33** 27
[19] Fernando G W, Watson R E and Weinert M 1992 Heats of formation of transition-metal alloys: Full-potential approach and the Pt-Ti system *Phys. Rev. B* **45** 15 8233